Cloning and Functional Characterization of a Formin-Like Protein (AtFH8) from Arabidopsis[1]

Kexi Yi, Chunqing Guo, Ding Chen, Binbin Zhao, Bin Yang, and Haiyun Ren*

Key Laboratory of Cell Proliferation and Regulation Biology of Ministry of Education, and College of Life Science, Beijing Normal University, Beijing 100875, People's Republic of China

The actin cytoskeleton is required for many cellular processes in plant cells. The nucleation process is the rate-limiting step for actin assembly. Formins belong to a new class of conserved actin nucleator, which includes at least 2 formin homology domains, FH1 and FH2, which direct the assembly of unbranched actin filaments. The function of plant formins is quite poorly understood. Here, we provide the first biochemical study of the function of conserved domains of a formin-like protein (AtFH8) from Arabidopsis (*Arabidopsis thaliana*). The purified recombinant AtFH8(FH1FH2) domain has the ability to nucleate actin filaments in vitro at the barbed end and caps the barbed end of actin filaments, decreasing the rate of subunit addition and dissociation. In addition, purified AtFH8(FH1FH2) binds actin filaments and severs them into short fragments. The proline-rich domain (FH1) of the AtFH8 binds directly to profilin and is necessary for nucleation when actin monomers are profilin bound. However, profilin inhibits the nucleation mediated by AtFH8(FH1FH2) to some extent, but increases the rate of actin filament elongation in the presence of AtFH8(FH1FH2). Moreover, overexpression of the full-length AtFH8 in Arabidopsis causes a prominent change in root hair cell development and its actin organization, indicating the involvement of AtFH8 in polarized cell growth through the actin cytoskeleton.

The actin cytoskeleton of plant cells is temporally and spatially regulated in response to external stimuli and plays an important role in many physiological processes, like cytoplasmic streaming, division plane coordination, and tip growth (Volkmann and Baluska, 1999; Staiger et al., 2000). A host of accessory proteins are required to regulate the equilibrium between monomeric G-actin and F-actin, to bundle and cross-link actin filaments to one another, or to promote nucleation of new actin filaments (Ayscough, 1998). The formation of actin trimers, the smallest nuclei for polymerization, is the rate-limiting step during spontaneous filament assembly. Thus, cellular activities that either block or stimulate trimer formation have a large influence on actin polymerization (Cooper et al., 1983; Winter et al., 1997). Relatively recent studies have provided important new insights into how the assembly and disassembly of the actin cytoskeleton is regulated. The Arp2/3 complex has been demonstrated as a nucleation factor in the stimulation of branched filament formation (for review, see Pollard and Beltzner, 2002). Recently, a conserved family of formin homology proteins has emerged as a new class of actin nucleator that directs assembly of straight filaments independently of the Arp2/3 complex (for review, see Zigmond, 2004).

Formins are large multidomain proteins that have been found in all eukaryotes examined and are required for multiple actin-related processes, such as cytokinesis and maintenance of cell polarity, in many organisms (Wasserman, 1998; Sawin, 2002). The mouse *limb deformity* gene encodes the first formin identified. Subsequently, additional genes encoding formins have been found in fungi, plants, worms, and mammals. All formins contain a unique, highly conserved formin homology domain, FH2, which interacts with actin, and a domain rich in Pro-FH1 located N terminally to the FH2 domain, which binds to the actin-associated protein profilin. Some formins from animals and fungi also contain a third FH domain, FH3, a loosely conserved domain that determines appropriate subcellular localizations of formins, a GTPase-binding domain located at the N terminal, and diaphanous-autoregulatory domain at the C terminal of formins (for review, see Evangelista et al., 2003). Evidence as to the effect of formins on actin polymerization has been obtained using FH1/FH2 constructs of various lengths from different formins (Pruyne et al., 2002; Kovar et al., 2003; Li and Higgs, 2003; Harris et al., 2004). When incubated in vitro with pure actin, recombinant fragments of FH2 are necessary and sufficient to nucleate actin filaments anchored at the barbed end, and FH1FH2 behaves similarly to FH2. However, FH1FH2 can stimulate the nucleation by utilizing profilin-actin, although it is less effective at enabling nucleation than free G-actin (Pruyne et al., 2002; Sagot et al., 2002; Kovar et al., 2003; Li and Higgs, 2003). The mechanism of actin nucleation studied with the Bni1p

[1] This work was supported by the National Science Foundation for Distinguished Young Scholars (grant no. 30325005 to H.R.) and the National Natural Science Foundation of China (grant no. 30470176 to H.R.).

* Corresponding author; e-mail hren@bnu.edu.cn; fax 86–10–58807721.

Article, publication date, and citation information can be found at www.plantphysiol.org/cgi/doi/10.1104/pp.104.055665.

FH2 domain suggests that FH2 domain stabilizes an actin dimer and that this complex functions as a nucleation unit. FH1FH2 also competes with tight capping proteins for the barbed end but still allows elongation of actin filaments.

The Arabidopsis (*Arabidopsis thaliana*) genome contains at least 21 formin genes that have been divided into 2 classes: group I and group II, defined by the presence or absence of an N-terminal transmembrane domain (Banno and Chua, 2000; Cvrčková, 2000; Deeks et al., 2002) that does not appear in formins from other organisms. Recently, results from overexpression of the Arabidopsis formin AFH1 in pollen suggest that AFH1-regulated actin polymerization is important for polar pollen cell growth (Cheung and Wu, 2004). However, little is known about the actin nucleation activity of plant formins. In this study, AtFH8, a group-I formin from the Arabidopsis 21-member formin gene family (Deeks et al., 2002) has been cloned, expressed, and characterized with the aim of understanding the role of plant formins on the process of actin assembly.

RESULTS

The Identification and Cloning of AtFH8

Arabidopsis cDNA sequences for putative FH proteins (formin homology proteins) were identified in The Arabidopsis Information Resource (TAIR) database and had been analyzed (Cvrčková, 2000; Deeks et al., 2002). In this study, we focused our efforts on AtFH8 (At1g70140), one of group I formins in Arabidopsis genome. AtFH8 is deduced from genomic sequence information obtained from the bacterial artificial chromosome clone F20P5 (AC002062). The cDNA sequence encoding AtFH8 reported to date was incomplete at the 3′ end (GenBank accession no. AY050956; National Center for Biotechnology Information [NCBI]). To obtain the full-length open reading frame of AtFH8, we performed reverse transcription (RT)-PCR by using total RNA from 10-d-old Arabidopsis seedlings as a template to amplify a cDNA encoding the entire Arabidopsis AtFH8. The amino acid sequence deduced from the full-length cDNA was identical to that predicted in TAIR database. The protein predicted from this cDNA contains 760 amino acid residues and has an estimated molecular mass of approximately 83.6 kD and pI of 9.54. When conducting a conserved domain search in NCBI Conserved Domain Database (CDD; Marchler-Bauer et al., 2003), the 296-721 amino acid of AtFH8 is highly homological to Formin Homology 2 Domain (smart 00498) with 50.9% similarity of amino acid. Moreover, when compared with the equivalent region of submitted sequences in the NCBI CDD, AtFH8 shares 38.2% identity with members of the Rho GTPase effectors BNI1 and related formins, 25.1% identity to Diaphanous-related formins, and 28.4% identity to formin-related protein in leukocytes (FRLs; Fig. 1). Among all 21 Arabidopsis formins, a TAIR Fasta search revealed that AtFH8 shows the highest identity of 67.4% with AtFH4 (At1g 24150). When compared with AFH1 (At3g 25500) and AtFH6 (At5g 67470), the only ones studied experimentally (Banno and Chua, 2000; Cheung and Wu, 2004; Favery et al., 2004), AtFH8 shares 36.6% and 33.2% identity to them, respectively. The N-terminal region of AtFH8 has a Pro-rich region and a transmembrane domain, which were well analyzed in AFH1 and AtFH6 (Banno and Chua, 2000; Cvrčková, 2000; see Fig. 2A). From the analysis described above, it can be concluded that AtFH8 obtained represents a member of Arabidopsis formin family proteins.

Generation of Recombinant AtFH8 Truncated Proteins

To investigate the interactions of FH1 and FH2 domains of AtFH8 with G-actin and actin filaments, 2 deletion constructs, named AtFH8(FH1FH2) and AtFH8(FH2), were designed from the AtFH8 sequence and used in this study (depicted in Fig. 2A). The truncated proteins were expressed as His-tagged forms in *Escherichia coli*. Using nickel-nitrilotriacetic acid agarose chromatography, we obtained about 2 mg of proteins with about 95% purity from 1-L cultures (Fig. 2B). The apparent molecular mass of AtFH8(FH2) is 56 kD, which is consistent with what is expected from sequence prediction (Fig. 2B, lane 3). However, the apparent molecular mass of AtFH8(FH1FH2) was 70 kD (Fig. 2B, lane 2), which was a bit higher than that expected (65 kD). To verify this protein, the protein band was excised from SDS-PAGE gel, digested with trypsin, and then analyzed by matrix-assisted laser-desorption ionization mass spectrometry. The source proteins were identified by peptide mass search against the NCBI database using Mascot software. The data obtained matched to the putative amino acid sequence of AtFH8 completely (data not shown),

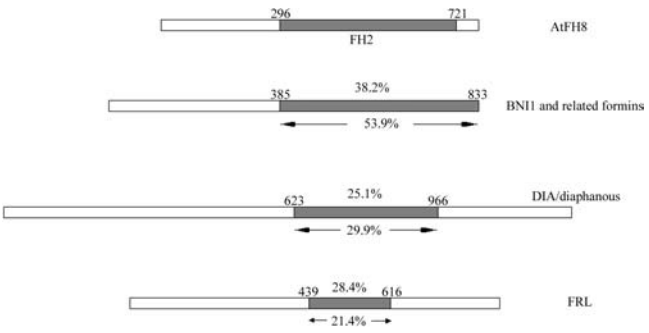

Figure 1. Schematic presentation of FH2 domain of AtFH8 and other formin-like proteins. The identity indicated above the bar was calculated by the ratio of the number of the identical amino acids to that of the corresponding amino acids of AtFH8 and the number below each bar indicates the percentage of sequence aligned in the search. The marked region of each formin indicates the alignment area when conducting the blast.

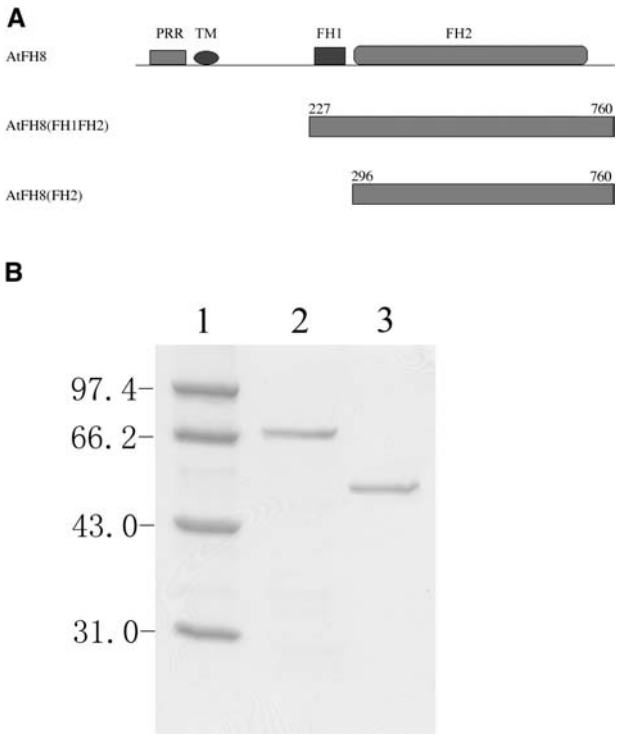

Figure 2. Domain organization of AtFH8 deletion constructs and purification of AtFH8 truncated proteins. A, Schematic domain maps of AtFH8 and AtFH8 constructs used in this study. PRR, Pro-rich region; TM, transmembrane domain; FH1 and FH2, formin homology domain 1 and 2, respectively. Numbers over each construct indicate amino acid residues that it contains. B, Coomassie-Blue stained SDS-PAGE gel of AtFH8 truncated proteins used in this study. Lane 1, M_r marker; lane 2, AtFH8(FH1FH2); lane 3, AtFH8(FH2).

indicating that the recombinant AtFH8(FH1FH2) was correctly expressed. However, the reason for the improper apparent molecular mass remains unknown.

AtFH8(FH1FH2) Nucleates Actin Assembly and Decreases the Critical Concentration of Actin Assembly

To investigate the function of AtFH8(FH1FH2) domain on actin assembly, experiments to examine the effect of AtFH8(FH1FH2) on the kinetics of actin polymerization were performed by light scattering measurement (Fig. 3). The results showed that the polymerization of actin alone was initially slow, reflecting a slow spontaneous nucleation activity of purified actin monomers. However, after the addition of the recombinant AtFH8(FH1FH2), actin polymerization was accelerated, and the nucleation activity could be enhanced with increased AtFH8(FH1FH2) concentrations (Fig. 3A). In addition, we also found that the ability of AtFH8(FH1FH2) to accelerate polymerization was dependent on the concentration of actin monomers (Fig. 3B). Increasing monomer concentration over a range from 1 μM to 7 μM caused an exponential increase in the concentration of filaments assembled.

To examine the amount of actin polymerization at steady state in the presence of AtFH8(FH1FH2), sedimentation assays were performed. As shown in Figure 4A, samples with the addition of AtFH8(FH1FH2) contained 3.48 $\pm$ 0.89-fold (mean $\pm$ SE; $n = 3$) more actin filaments in pellets than when AtFH8(FH1FH2) was not added during the first 5 min and was opposite to that found in supernatant; after 16 h incubation, samples with the addition of AtFH8(FH1FH2) contained 1.15 $\pm$ 0.03-fold (mean $\pm$ SE; $n = 3$) more actin filaments in the pellets than actin control, indicating the difference between the pellets was much less by this time. As seen from the supernatant, in the sample after 16 h incubation, there was more G-actin in the control sample, indicating that AtFH8(FH1FH2) decreased the critical concentration of actin polymerization. To determine the critical concentration (Cc) shifted by AtFH8(FH1FH2), a series of different

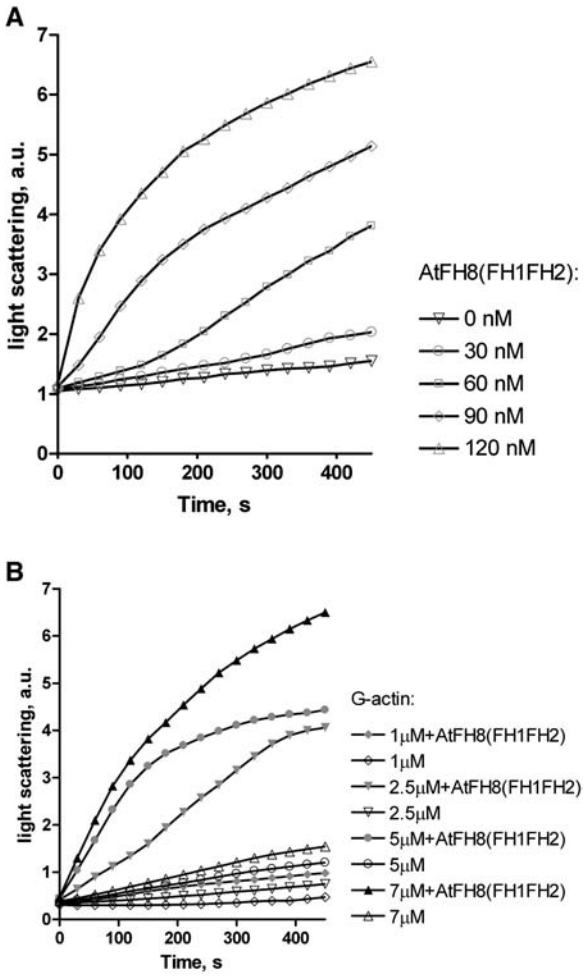

Figure 3. AtFH8(FH1FH2) nucleates actin filaments in vitro. A, Time course of the polymerization of actin (3 μM) was monitored by light scattering in the presence of the indicated concentrations of AtFH8(FH1FH2). B, AtFH8(FH1FH2)-induced actin assembly shows G-actin dose dependence. Actin assembly assay was performed with different concentrations of actin in the presence or absence of 90 nM AtFH8(FH1FH2).

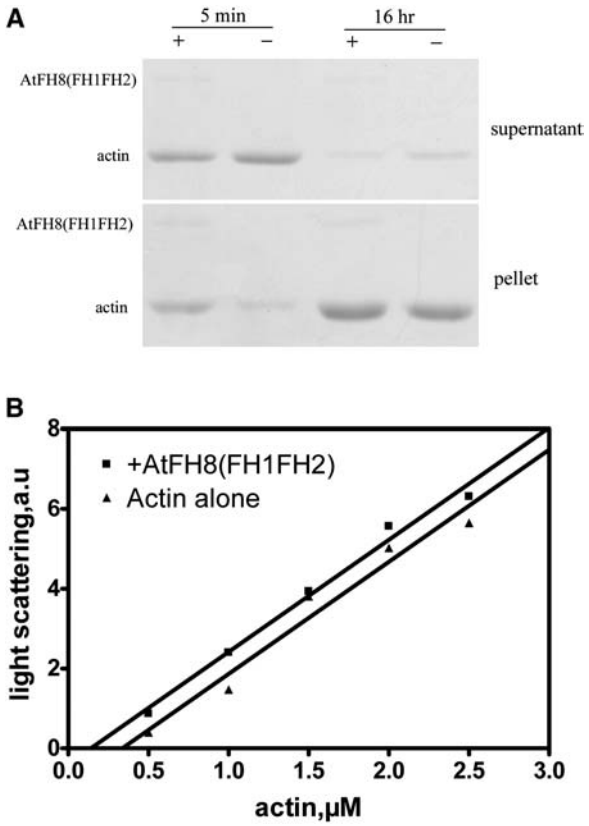

Figure 4. Examination of the effect of AtFH8(FH1FH2) on critical concentration of actin polymerization. A, Actin (3 μM) was polymerized and pelleted by ultracentrifugation at different time points in the presence or absence of 80 nM AtFH8(FH1FH2). "+" indicates the presence of AtFH8(FH1FH2), and "−" indicates the absence of AtFH8(FH1FH2). B, Different concentrations of actin were incubated in the absence or presence of 80 nM AtFH8(FH1FH2) and allowed to polymerize for over 16 h at room temperature. The figure is a representative experiment with Cc (*x* axis intercept of each regression line) of 0.24 μM for actin alone and Cc of 0.16 μM for actin in presence of AtFH8(FH1FH2).

concentrations of actin was used for actin polymerization in the presence of 80 nM AtFH8(FH1FH2) monitored by light scattering measurement. As shown in Figure 4B, 80 nM AtFH8(FH1FH2) shifted Cc from 0.33 ± 0.10 to 0.19 ± 0.06 μM (mean ± SD; $n = 5$).

AtFH8(FH1FH2) Partially Caps Filament Barbed End and Slows the Elongation Rate of Actin Filaments

It has been shown that several formins such as mDia, Bnilp, and cdc12p have barbed-end capping activity on actin filaments (Pruyne et al., 2002; Kovar et al., 2003; Li and Higgs, 2003). Because the rate of depolymerization from barbed ends is more than 20-fold faster than that from pointed ends, the reduction of the depolymerization rate reflects the barbed-end capping activity (Pollard, 1986). Thus, a depolymerization assay was used to examine the capping activity of AtFH8(FH1FH2) by light scattering measurement. Compared to the controls, the rate of depolymerization of actin filaments in the presence of AtFH8(FH1FH2) decreased in a dose-dependent manner, indicating the capping activity of AtFH8(FH1FH2) on actin filament barbed ends. However, 200 nM AtFH8(FH1FH2) still could not fully cap the barbed end (Fig. 5A), indicating that AtFH8(FH1FH2) could only partially cap the barbed ends of actin filaments. To test if this capping activity affected the elongation rate of the filament, phalloidin-stabilized actin seeds generated by shearing preformed actin filaments through a syringe were used for measuring the elongation rate in the presence of AtFH8(FH1FH2). As shown in Figure 5B, AtFH8(FH1FH2) inhibited actin filament elongation in a dose-dependent manner and slowed down the elongation rate maximally to one-sixth of purified actin alone. The one-half-maximal inhibition indicated a dissociation constant (*K*d) of 18.2 nM. These results further support the idea that AtFH8(FH1FH2) caps actin filaments partially and allows the elongation of the actin filaments from the barbed end.

AtFH8(FH1FH2) Binds and Severs Actin Filaments

The ability of recombinant AtFH8(FH1FH2) to bind to F-actin was assayed using a high-speed cosedimentation assay. As shown in Figure 6A, in the absence of F-actin, very little AtFH8(FH1FH2) was sedimented (Fig. 6A, lane 4), which may be due to misfolding or aggregation of the bacterially expressed protein products. However, a significant amount of AtFH8(FH1FH2) cosedimented with polymerized actin, and the amount of AtFH8(FH1FH2) in the pellets increased with increasing actin filament concentration (Fig. 6A, lanes 1–3). When plotting the concentration of AtFH8(FH1FH2) in the supernatants or pellets against concentrations of actin filaments, the intersection of the 2 curves suggests that 50% of AtFH8(FH1FH2) binds to actin filaments; thus, this actin concentration represents the apparent *K*d. Figure 6B is a representative of 5 measurements, and the mean value is about 0.69 ± 0.21 μM (mean ± SE; $n = 5$). The results indicated that AtFH8(FH1FH2) was able to bind to F-actin tightly. To examine whether this binding activity has other functions, such as bundling or severing, we observed the AtFH8(FH1FH2) nucleated filaments using electron microscopy. The result showed that the filaments were unbundled and unbranched (data not shown). Using a fluorescence microscopy assay, the severing activity of the recombinant AtFH8(FH1FH2) on F-actin was examined. It was found that after the addition of AtFH8(FH1FH2) to preformed actin filaments, there was a significant decrease in filament length observed (Fig. 6C). When the molecular ratio of AtFH8(FH1FH2):actin was 1:100, the length of resultant actin filaments decreased from about 13.29 ± 1.90 μm to 3.44 ± 0.46 μm (mean ± SE; calculated from 50 actin filaments). The severing activity of AtFH8(FH1FH2) was similar to FRLα-C (Harris et al., 2004), but has not been found from other formins previously described.

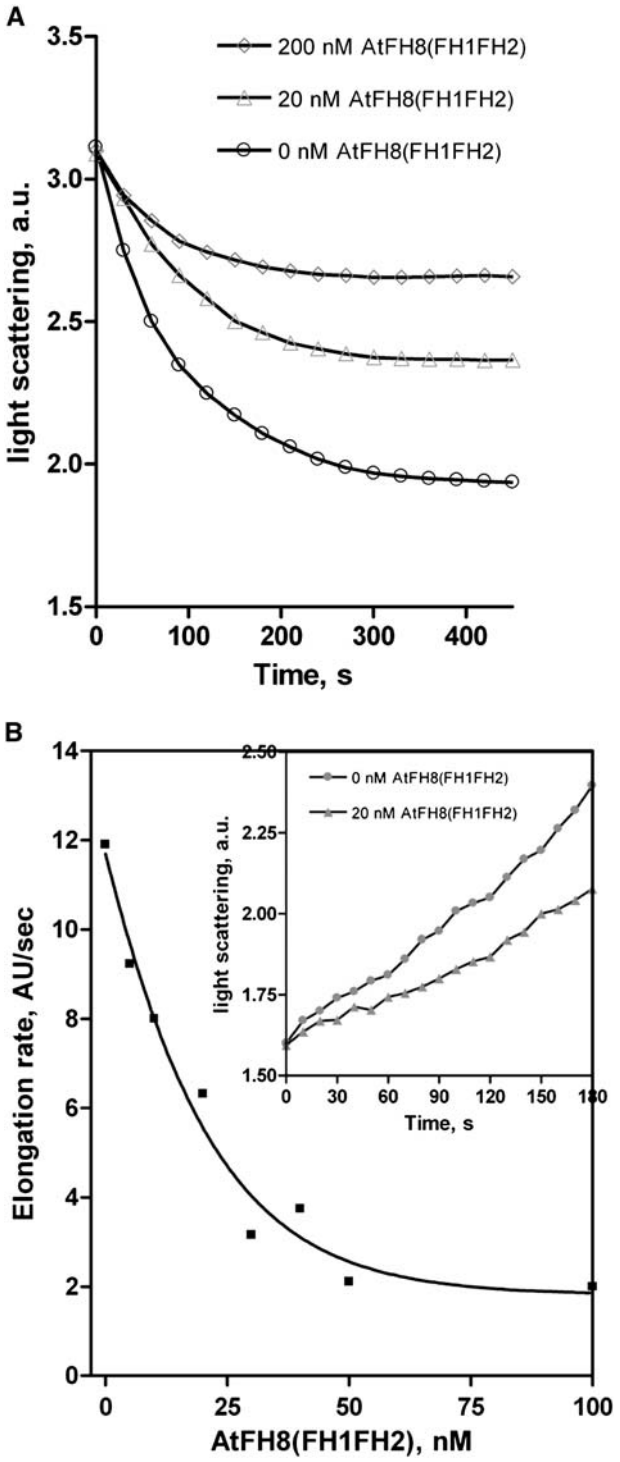

Figure 5. AtFH8(FH1FH2) partially caps filaments barbed ends and slows the elongation rate from this end. A, Effect of AtFH8(FH1FH2) on the actin filament depolymerization rate. Actin filaments were diluted to 0.1 μM in F-buffer alone or in the presence of either 20 nM or 200 nM AtFH8(FH1FH2). B, AtFH8(FH1FH2) slows the elongation rate from actin filaments barbed ends. Phalloidin-stabilized filaments seeds were incubated with varying concentrations of AtFH8(FH1FH2) and 0.5 μM G-actin was added to initiate actin elongation at the barbed end. The elongation rate was measured as the slope of the increase of the light scattering value for each concentration. Inset, Examples of the raw data with 0 or 20 nM AtFH8(FH1FH2).

FH1 Domain Is Crucial for AtFH8(FH1FH2) Effect on Profilin-Actin Polymerization

Profilin is a highly abundant actin monomer binding protein that inhibits actin nucleation and prevents monomer addition to filament pointed ends (Cooper and Pollard, 1985; Valenta et al., 1991; Staiger et al., 1997). Formins in other organisms have been shown to contribute to profilin-actin polymerization (Kovar et al., 2003; Pring et al., 2003). Thus, the effect of AtFH8(FH1FH2) on the profilin-actin nucleation process was investigated in this study. As shown in Figure 7A, the spontaneous polymerization of actin was inhibited by profilin. However, after the addition of AtFH8(FH1FH2), the polymerization was accelerated, indicating that AtFH8(FH1FH2) could accelerate the nucleation of profilin-actin. Furthermore, to determine whether the FH1 domain is a necessary domain for this effect, another construct, AtFH8(FH2), with 296-760 amino acids of AtFH8, was also used. The results showed that AtFH8(FH2) could accelerate the pure G-actin nucleation but could not accelerate the polymerization of profilin-actin complex (Fig. 7A), indicating that FH1 domain is crucial for AtFH8(FH1FH2) to regulate profilin-actin nucleation and polymerization. To examine whether FH1 domain directly binds to profilin, an affinity precipitation assay was performed. As shown in Figure 7B, AtFH8(FH1FH2) was precipitated by immobilized profilin, but AtFH8(FH2) was not. Quantitative analysis of the SDS-PAGE gels showed that 12.01 $\pm$ 1.58% (mean $\pm$ SE; $n = 3$) of AtFH8(FH1FH2) bound to the immobilized profilin. The results demonstrated directly that FH1 is required for the binding of the 2 proteins. The fact that AtFH8(FH2) nucleates actin suggests that FH2 domain of AtFH8 is sufficient for actin filament nucleation.

Profilin Increases Elongation Rate of Actin Assembly from Barbed End in the Presence of AtFH8(FH1FH2)

By using fluorescence microscopy, we further observed the effects of AtFH8(FH1FH2) and AtFH8(FH2) on the polymerization rate of actin or profilin-actin directly. After incubation of actin and 120 nM of AtFH8(FH1FH2) or AtFH8(FH2) in F-buffer for 5 min, the filament lengths were measured directly using microscopy. The filament lengths in controls (actin alone) were 21.60 $\pm$ 5.47 μm (mean $\pm$ SD; calculated from 60 of actin filaments, the same in the following; Fig. 8A, subsection a), but the lengths of actin filaments formed in the presence of AtFH8(FH1FH2) or AtFH8(FH2) were 5.38 $\pm$ 3.06 μm and 5.56 $\pm$ 2.30 μm, respectively (Fig. 8A, subsections c and e), which were much shorter than actin alone. These results directly demonstrated that both AtFH8(FH1FH2) and AtFH8(FH2) nucleated actin filaments grew slower than spontaneous polymerized actin did. In the presence of profilin, actin could not polymerize into visible filaments (Fig. 8A, subsection b), which might be due to the sequestering role of profilin to actin. When

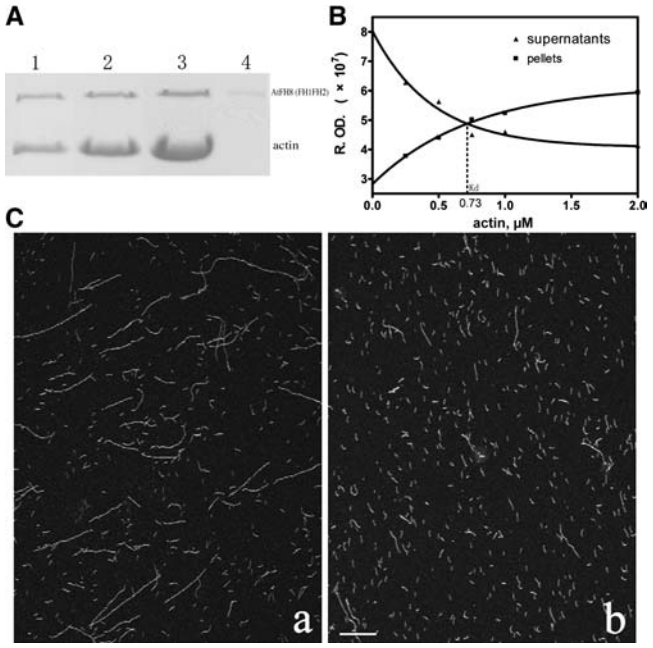

Figure 6. AtFH8(FH1FH2) binds and severs actin filaments in vitro. A, Coomassie-Blue stained SDS-PAGE of pelleting assays using 200 nM AtFH8(FH1FH2) with varying concentrations of actin filaments. Lane 1, 0.5 μM F-actin; lane 2, 1 μM F-actin; lane 3, 2 μM F-actin; lane 4, minus F-actin. B, Plot of relative gray value (R. OD) of AtFH8(FH1FH2) in Coomassie-Blue stained SDS-PAGE gel against actin concentrations from experiments conducted as described in Figure 6A. The R.OD of AtFH8(FH1FH2) in pellets is indicated by black squares and the supernatants is indicated by black triangles, the intersection of the two indicates that 50% of AtFH8(FH1FH2) binds to actin filaments. In this representative experiment, the apparent *K*d is 0.73 μM. C, AtFH8(FH1FH2) severs preformed actin filaments in vitro. After incubation with or without 30 nM AtFH8(FH1FH2) for 1 h, the preformed actin filaments (3 μM) were mixed with equal volume of 6.6 μM Alexa-phalloidin and diluted 20-fold into F-buffer before visualization. Bar = 15 μm.

AtFH8(FH1FH2) was added to actin-profilin in F-buffer, actin polymerized into even longer filaments (11.04 ± 4.38 μm; Fig. 8A, subsection d) than that with actin alone (Fig. 8A, subsections c and e). However, AtFH8(FH2) had no effect on profilin-actin complex polymerization (Fig. 8A, subsection f).

Furthermore, the elongation rate of the barbed end of actin or actin-profilin polymerization in the presence or absence of AtFH8(FH1FH2) was compared using phalloidin-stabilized filament seeds (described above). As shown in Figure 8B, in the absence of AtFH8(FH1FH2), the elongation rate of actin filaments in the presence of profilin is much lower than that of actin in the absence of profilin. However, in the presence of AtFH8(FH1FH2), the elongation rate of barbed ends from actin in the presence of profilin was much faster (about 2-fold) than that from G-actin alone. The reason was probably that the lengths of AtFH8(FH1FH2) nucleated actin filaments from actin in the presence of profilin were much longer than that from actin without profilin (Fig. 8A, subsection d), indicating that profilin might make it easier for actin to add to the barbed end in the presence of AtFH8(FH1FH2). These results suggested that profilin might serve as a regulator that facilitates the assembly of the barbed end of AtFH8(FH1FH2) nucleated actin filaments.

Overexpression of AtFH8 Affects the Root Hair Morphogenesis and Tip Growth

Formin family proteins have been implicated in playing essential roles in cell polarization (Evangelista et al., 1997; Ozaki-Kuroda et al., 2001; Sawin, 2002). Overexpression of AFH1 caused tube broadening, growth depolarization, and growth arrest in pollen tubes (Cheung and Wu, 2004). To study the function of AtFH8 in Arabidopsis, we generated transgenic plants overexpressing AtFH8 using the floral dip method. Expression levels of the transgene were detected by RT-PCR analysis of AtFH8 mRNA. Lines with an approximately 5- to 10-fold increase in mRNA expression level (data not shown) were selected for further analysis. It was found that overexpression of AtFH8 did not have any lethal effect or obvious phenotypic

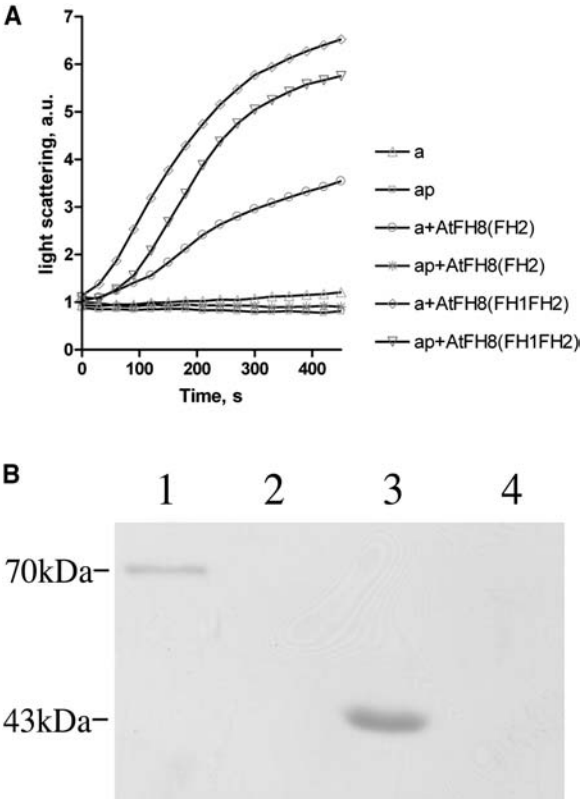

Figure 7. FH1 domain is crucial for the role of AtFH8(FH1FH2) to profilin-actin polymerization. A, AtFH8(FH1FH2) nucleates profilin-actin but AtFH8(FH2) does not. Actin or profilin-actin was induced to polymerize in the presence or absence of 120 nM AtFH8 truncated proteins. B, Affinity precipitation of AtFH8 truncated proteins with immobilized profilin. Lane 1, AtFH8(FH1FH2); lane 2, AtFH8(FH2); lane 3, actin as positive control; lane 4, BSA as negative control.

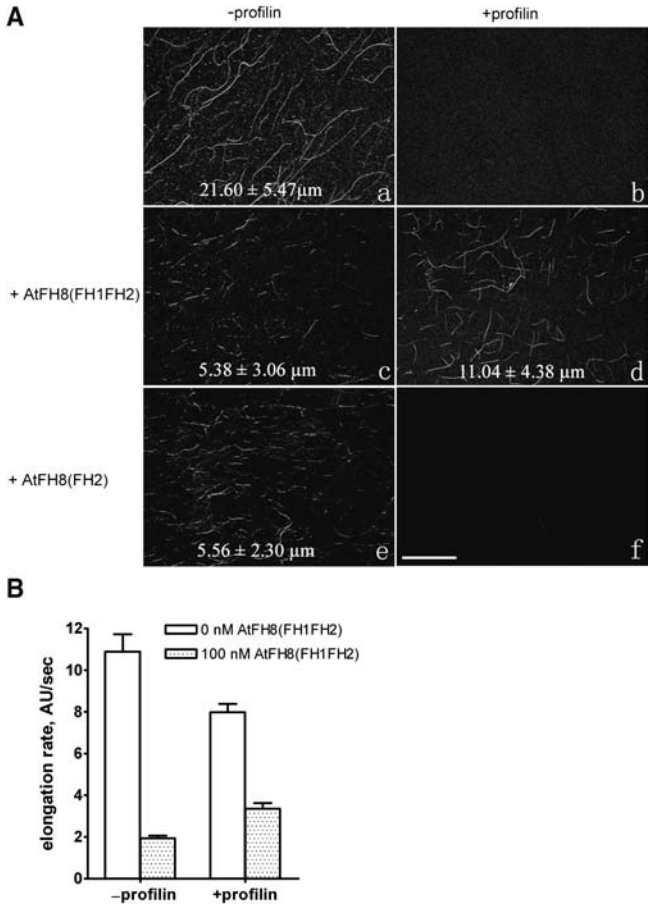

Figure 8. Effect of profilin on barbed-end actin assembly in the presence of AtFH8(FH1FH2). A, Fluorescence microscopy investigation of the role of AtFH8 truncated proteins on profilin-actin. Actin or profilin-actin was induced to polymerize in the presence or absence of AtFH8 truncated proteins for 5 min, then the filaments were visualized by labeling with Alexa-phalloidin immediately. The numbers indicate the average filament lengths (mean value ± SD). Bar = 15 μm. B, Profilin decreases AtFH8(FH1FH2) inhibition of actin filament elongation rate of barbed end. Elongation rates were measured as described in Figure 5B and the actin monomers (1 μM) was mixed with profilin (4 μM) in advance.

changes in stem or leaf epidermal cells (data not shown). However, it did lead to dramatic changes in root hair development (Fig. 9). AtFH8-overexpressing plants showed various phenotypes. A relatively weak phenotype had short hairs (Fig. 9b), wavy hairs (Fig. 9c), or swelling root tips (Fig. 9d). An intermediate phenotype had branched root tips with different repeats (Fig. 9, e–i). Stronger phenotypes initiated two hairs on one hair-forming site in individual cells (Fig. 9, j and k), and even formed bulbous structures at the root hair bases (Fig. 9l). Similar phenotypes were observed in all other AtFH8-overexpressing lines (data not shown), indicating that the phenotypes are caused by AtFH8 overexpression. However, the position and numbers of root hair were not obviously altered; like wild-type lines, AtFH8-overexpressing lines usually have one hair-forming site in each hair-forming cell, and the hair is usually close to the end of the cell nearest the root tip (data not shown). In addition, the number of hairs <40 μm in length per millimeter was much higher in AtFH8-overexpressing plants than in wild types and the length of the root hairs in AtFH8-overexpressing plants was shorter than in wild-type plants (Table I). Because it was thought that wild-type root hairs complete the transition to tip growth before they reach 40 μm in length (Dolan et al., 1994), these results suggest that AtFH8 is involved in both bulge initiation and the tip growth of root hairs.

Overexpression of AtFH8 Alters the Distribution of Actin Cytoskeleton in Root Hairs

It is well known that actin cytoskeleton plays a key role in controlling tip growth of root hairs. To determine if AtFH8 is involved in the process, we generated transgenic plants overexpressing AtFH8 in transgenic GFP-mTalin Arabidopsis lines (gifts from Dr. Ming Yuan), which express GFP-mTalin (green fluorescent mouse talin fusion protein) that binds specifically to filamentous-actin (McKann and Craig, 1997; Kost et al., 2000), to visualize actin filaments in living root hair cells. As shown in Figure 10, the actin filaments were located in a net-axial orientation more

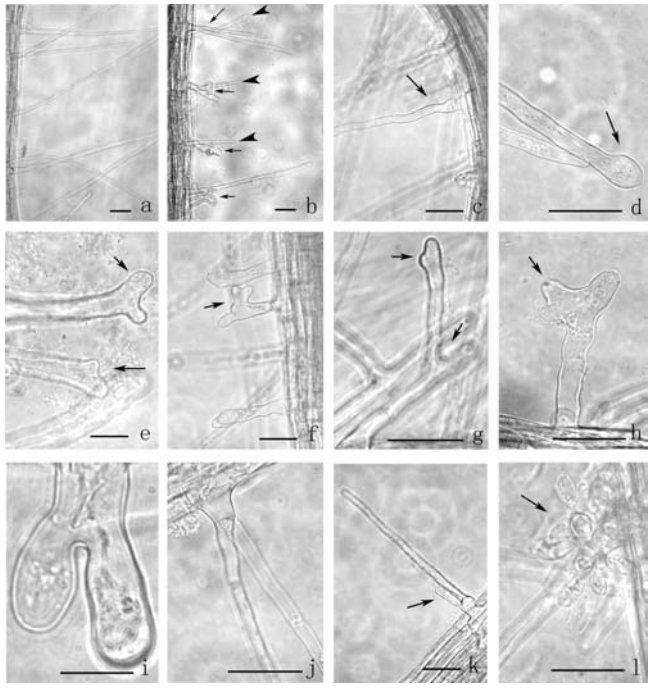

Figure 9. Root hair phenotypes of AtFH8-overexpressed plants. AtFH8 overexpression affects root hair phenotypes and root hair tip growth. a, Wild-type root hairs. b to l, AtFH8-overexpressing root hairs. b, Overview of AtFH8-overexpressing root hair phenotypes with arrowheads showing shorter root hairs, (c) wavy root hair, (d) swelling tip of root hair, (e–i) different degrees of branched root hairs, (j and k) 2 root hairs from one hair-forming site, and (l) bulbous structure at root hair basis. Arrows show root hair phenotypes. Bars = 50 μm, except in i, bar = 20 μm.

Table I. *AtFH8 affects length of root hair*

Hairs <40 μm were counted in the 1-mm region length at the midpoint of a root. From the same region, the length of 10 full-expanded root hairs (all > 40 μm) were randomly selected and measured. Altogether, eight roots were measured.

Arabidopsis Lines	No. of Hairs <40 μm	Length of Mature Root Hairs (Root hairs <40 μm were excluded)
		μm
WT	3.0 ± 1.07	465.9 ± 62.37
AtFH8	6.0 ± 2.88	364.9 ± 48.42

or less parallel to the long axis of the tube and the actin cables reached just to the subapical region of root hairs in wild-type/GFP-mTalin line (Fig. 10a). However, in root hairs of AtFH8/GFP-mTalin plants, the fluorescence of actin filaments was much brighter, indicating that there were more actin filaments in root hairs of AtFH8/GFP-mTalin plants. Actin filaments displayed thick spiral actin cables reaching to the extreme apical region in some normal shaped root hairs (Fig. 10b) of the weak phenotype. But, in other root hairs of weak phenotype, besides the existence of actin cables reaching to the extreme apical region, there also existed actin patches or finer actin networks (which cannot be clearly distinguished using fluorescence microscopy) in the root hair (Fig. 10, c and d). However, in the root hairs of intermediate and stronger phenotypes, the actin filaments showed very irregular configuration: actin filaments formed polygonal meshes seemingly surrounding some kinds of organelles in whole root hair tubes with multiple tips (Fig. 10e) or initiated from one hair-forming site (Fig. 10f), but there were less actin bundles along the long axis of the tube of these kinds of root hairs. All lines detected showed similar results. These observations strongly support a role that AtFH8 played in the regulation of actin cytoskeleton during the initiation and tip-growth process of root hairs.

DISCUSSION

The Role of Formin from Plant Cells Is Highly Conserved to the Formin from Other Organisms in Vitro

Formins from many organisms have been found to nucleate actin filaments. Although a number of formin-like sequences from Arabidopsis and other plant species are present in the gene databases, little is known about their biochemical properties and their role in the regulation of dynamics of actin polymerization. In this study, we isolated cDNAs identified in TAIR database encoding a full length of formin protein-AtFH8, FH2 domain, and FH1FH2 domain of AtFH8. The structure of AtFH8 is similar to that of AFH1 identified by Chua's group (Banno and Chua, 2000). AtFH8 contains FH1, FH2, and a putative transmembrane domain and extracellular domain in the N terminal, but no FH3, GTPase-binding domain, and diaphanous-autoregulatory domain typically found in formins of animals and fungi (Evangelista et al., 1997; Alberts, 2001; Palazzo et al., 2001). Because the effects of formins on actin polymerization were demonstrated through FH2/FH1 domain, constructs of various lengths from different formins and both glutathione *S*-transferase (GST)-Bni1pFH1FH2 lacking the COOH-terminal extension and purified Bni1pFH1FH2 lacking the GST tag have been demonstrated to have nucleation activity similar to that of GST-Bni1pFH1FH2-COOH (Pruyne et al., 2002; Li and Higgs, 2003), we expressed FH2 and FH1FH2 constructs to find out the functional activities of the FH1 and FH2 domains of AtFH8. We used rabbit skeletal muscle actin in our biochemical experiments because both animal and plant actin perform similar biochemical properties and polymerization kinetics, and large-scale preparations of rabbit skeletal muscle actin are easy to obtain (Ren et al., 1997; Huang et al., 2003). Our results showed that the recombinant Arabidopsis formin proteins, both AtFH8(FH1FH2) and AtFH8(FH2), nucleate actin filaments and bind to F-actin barbed end as a leaky cap, and this binding activity partially inhibits elongation rate from actin filaments barbed end. Our study also demonstrated that AtFH8(FH1FH2) can

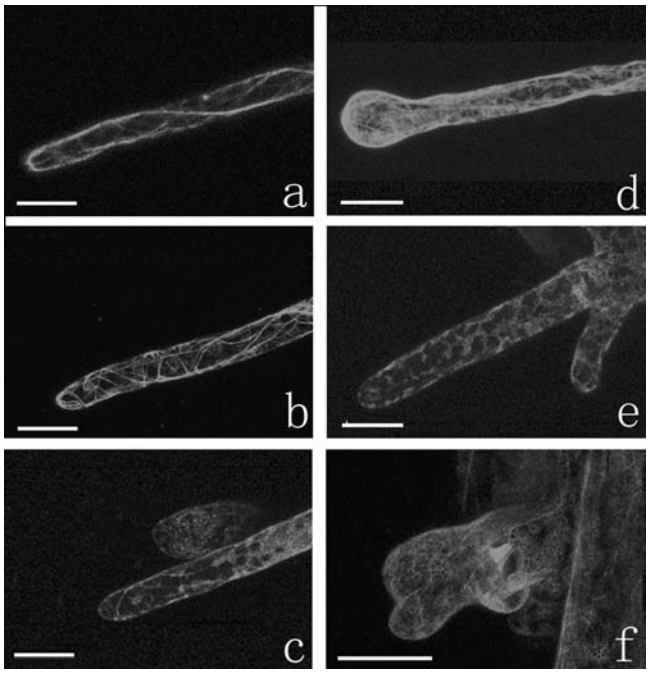

Figure 10. Effects of AtFH8-overexpression on F-actin in root hairs. a, Distribution of actin filaments in root hair of GFP-mTalin transgenic plant. b to f, Distribution of actin filaments in root hairs of AtFH8/GFP-mTalin overexpressing plants: b and c, actin filaments in normal shaped root hairs; d, actin filaments in root hair with swelling tip; e, actin filaments in branched root hair; and f, actin filaments in bulbous root hair. Pictures represent the projection of serial confocal optical sections. Bar = 20 μm.

bind to F-actin and sever actin filaments into short fragments. This severing ability has been found in just a few formins studied, so it might only belong to some special formins (Harris et al., 2004). In addition, it is shown that AtFH8(FH2) is an efficient nucleator of actin filament formation from monomers and reduces the lag period prior to actin assembly. These results agree in general with the findings in other members of this ubiquitous class of ABPs (Pruyne et al., 2002; Li and Higgs, 2003; Harris et al., 2004). Comparison of Arabidopsis FH2 domain sequences with the sequence of Bni1p reveals that Arabidopsis formins have specific features in Class I formins, but they may still form dimers and participate in actin nucleation (Cvrčková et al., 2004). All these support the idea that formins from many organisms share similar nucleation models.

Moreover, our work demonstrated the critical role of FH1 domain in mediating the interaction between AtFH8 and profilin-actin. Our affinity precipitation results show AtFH8(FH1FH2) can bind to profilin, but it is not the case with AtFH8(FH2); thus, we propose that AtFH8 interacts with profilin via the FH1 domain directly. The results are expected because profilin can bind to a number of Pro-rich domains. Subsequent studies demonstrated that this interaction plays a key role for AtFH8(FH1FH2) to nucleate profilin-actin and regulate profilin-actin to the barbed end. The observation on the lengths of actin filaments using fluorescent microscopy showed that in the presence of AtFH8(FH1FH2), profilin can help to nucleate the actin filaments. Considering the longer filaments formed by AtFH8(FH1FH2) on profilin-actin than on actin controls, we can conclude that profilin may serve as a regulator that facilitates the assembly of the barbed end of AtFH8(FH1FH2) nucleated filaments. Although we also tried to overexpress the recombinant AtFH8 by using pET and pGEX expression systems, this was not successful. It might be caused by the N-terminal structure of AtFH8, which may have a negative effect on the host cells (Soo et al., 2000). Our work represents an important step in the description and functional analysis of conserved actin-nucleating machinery in the plant kingdom.

AtFH8 Is Involved in the Process of Initiation and Tip Growth of Root Hairs

Root hair cells are specialized root epidermal cells with tubular extensions whose development, together with pollen tubes, serves as an excellent model to study the mechanism of tip growth of plant cells. Root hair development starts with an initial bulge formation at the distal end of the cell and then completes the transition to tip growth before they reach 40 μm in length (Dolan et al., 1994). In this study, we showed that overexpression of AtFH8 may induce more than one hair on each hair-forming site and that the number of hairs $<$40 μm in length per millimeter was much higher in AtFH8 overexpressing plants than in wild types, suggesting that AtFH8 is involved in the formation of initial bulge. In addition, we also presented evidence that suggests that AtFH8 may be involved in the process of tip growth, such as the formation of multiple tips from the same root hair and the short root hair phenotype in AtFH8 overexpression. Combining the above results and our data showing that the position and numbers of root hair were not obviously altered in AtFH8-overexpressing plants, we can conclude that AtFH8 is involved in both initiation and tip growth of the root hairs but is not involved in the selection of the bulge forming site.

The actin cytoskeleton plays a major role in root hair development (Volkmann and Baluska, 1999; Ringli et al., 2002). Application of actin filament-interfering compounds leads to aberrant root hair initiation, branched root hairs, and to cessation of the tip growth process during root hair elongation (Braun et al., 1999; Miller et al., 1999; Baluska et al., 2000). Here, we show that overexpression of AtFH8 induces more actin filaments, including actin cables reaching to the tip of the root hairs that display weak phenotypes, the actin filament network seemingly growing from the plasma membrane and some types of organelles that make the actin filaments form irregular configurations distributed in whole root hairs that display intermediate and stronger phenotypes. Based on bioinformatic analysis, AtFH8 may also be a microsomal membrane-associated protein as AtFH1 is (Banno and Chua, 2000). The reaching of actin bundles to the extreme tip region may be responsible for the short root hairs, because a fine actin meshwork needs to exist in the apex for normal tip growth (Baluska et al., 2000). Networks of actin filaments may be responsible for the multitip formation, which is consistent with the hypothesis that the configuration of actin in the apical area in plant and fungal tip-growing cells serves as a guidance mechanism for the secretory vesicles, the release of which into the expanding cell wall represents the cellular growth process (for review, see Geitmann and Emons, 2000; Staiger, 2000). These results are also consistent with the in vivo function analysis of AFH1 that transient expression of AFH1 induced supernumerary actin cable formation and resulted in polar growth changes in pollen tubes (Cheung and Wu, 2004). Our results suggest that AtFH8 affects the development of root hair cells through regulation of the actin cytoskeleton. Combining our in vivo and in vitro experiments, we postulate that overexpression of AtFH8 leads to more monomer actin recruited to form more actin filaments, which affects at least two stages: initiation and tip growth of the root hairs.

The functions of some formin family protein in animals and yeasts are regulated by Rho small GTPases (for review, see Zigmond, 2004). For example, in budding yeast, Bni1p is regulated by Rho1p in controlling the cell polarity (Tolliday, 2002). Plant members of the Rho family protein also play a critical role in controlling tip growth of plant cells (Fu et al., 2001; Molendijk et al., 2001). Recent studies have shown that

Rop2, a member of Rho family GTPase in Arabidopsis, acts as a positive regulatory switch in the bulge formation and in tip growth. Interestingly, AtFH8 overexpression caused some root hair phenotypes similar to the phenotypes induced by overexpression of Rop2 (Jones et al., 2002), such as individual hairs with multiple tips, but other root hair phenotypes distinct from the phenotypes induced by Rop2 overexpression, such as Rop2 overexpression, led to multiple hairs forming on individual cells while AtFH8 overexpression did not (Jones et al., 2002). Besides, Rop2 and AtFH8 appear to have an opposite function in root tip growth: Rop2 overexpressing plants have much longer hairs, but AtFH8 overexpressing plants have much shorter hairs than wild-type plants do. Therefore, it is not clear if Rop2 and AtFH8 act in the same pathway or in 2 distinct pathways to control the polarity of root hair tip growth. In addition, according to Kost et al. (1999), profilin might be involved in mediating the Rho regulated cytoskeleton process during the polar growth (Kost et al., 1999). Our biochemical results support that profilin acts as an interacting factor between AtFH8 and actin. However, the precise relationship between Rho, formin, profilin, and actin cytoskeleton needs to be further studied. Our results confirm and extend our understanding of the role of the formin family protein in plant cells.

MATERIALS AND METHODS

Plant Materials and Growth Conditions

Arabidopsis (*Arabidopsis thaliana*) ecotype Columbia wild-type seeds or transgenic seeds were surface sterilized and kept at 4°C for 3 d under dim light to aid germination. The seeds were plated on media containing 1% (w/v) agarose, 3% (w/v) Suc, and 1× Murashige and Skoog, pH 5.8. Subsequent growth was in a photoperiod of 16 h of light at 22°C and 8 h of darkness at 18°C. Hygromycin sensitivity was assayed on Murashige and Skoog plates using 40 μg mL^{-1} hygromycin. Ten days after germination, the seedlings were harvested for RNA extraction or DNA extraction.

Cloning and Sequencing of AtFH8 cDNA

A pair of primers, P8f (CCGGGATCC***ATG***GCTGCCATGTTTAAT; *Bam*HI site underlined) and P8r (GCGCGTCGAC***TCA***CATATCAGAATCCGA; *Sal*I site underlined), was designed from the coding region of the putative AtFH8 gene (TAIR database). The primers were used to perform reverse transcriptase mediated RT-PCR on total RNA from the seedlings of Arabidopsis using the Invitrogen RT-PCR system according to the manufacturer's instructions (Invitrogen, San Diego). The obtained 2,283-bp open reading frame of AtFH8 cDNA was cloned into pGEM-5Z (Promega, Madison, WI) and sequenced.

DNA Constructs and the Expression of the Recombinant AtFH8 Truncated Proteins

FH1FH2 coding region or FH2 coding region fragments of AtFH8 were amplified from cloning vector with *Pfu* polymerase (Stratagene, La Jolla, CA) and cloned in frame with 6×His in pET-30 a(+) vector (Novagen, Madison, WI). The resulting clones were sequenced to ensure the in-frame fusion and to avoid clones that contain mutations introduced by PCR.

For the expression of AtFH8 constructs, *Escherichia coli* strain BL21 (DE3; Novagen, Madison, WI) transformed with expression constructs was grown to OD 0.6 in Luria-Bertani medium. Then the fusion proteins were induced by 0.5 mM isopropylthio-β-galactoside at 37°C for 4 h, and the bacterial cells were pelleted and resuspended in a buffer containing 400 mM NaCl, 40 mM phosphate buffer saline, pH 8.0. The expressed proteins were purified using a Ni^{2+} column according to manufacturer's manual (Novagen). All proteins were dialyzed against TK buffer (5 mM Tris, 50 mM KCl, 0.5 mM dithiothreitol, 0.5 mM EDTA, and 5% glycerol) and stored in aliquots in liquid nitrogen. Protein concentrations were determined with the Bradford reagent (Bio-Rad, Hercules, CA), using bovine serum albumin (BSA) as a standard.

Protein Identification by Peptide Mass Fingerprinting

After 12% SDS-PAGE, band of interest was excised from the gel followed by destaining, reduction, alkylation, and further hydrolyzed with modified porcine trypsin as described by Hellman et al. (1995). Samples for MALDI-time of flight analysis were prepared by mixing a small aliquot of the digestion supernatant with equal volume of 4-hydroxy-α-cyano-cinnamic acid. Peptide mass fingerprinting was performed on the MALDI-time of flight (Autoflex, Bruker Instruments, Billerica, MA). A peak list was compiled with the *m/z* software (Proteometrics, New York) and used for peak selection. The peptide masses were used in a search against the NCBI database using Mascot software (Matrix Science, London).

Actin Assembly Assays by Light Scattering

Rabbit skeletal muscle actin prepared by the methods described by Pardee and Spudich (1982) in G-buffer (5 mM Tris-HCl, pH 8.0, 0.1 mM $CaCl_2$, 1 mM dithiothreitol, and 0.05 mM ATP) was precleared at 150,000*g* for 1 h before use. To examine the nucleating activity of AtFH8(FH1FH2), we detected its effect on the initial phase of actin polymerization. Actin with or without various concentrations of AtFH8(FH1FH2) was polymerized by adding 1/10 volume of 10× F-buffer (G-buffer with the addition of 500 mM KCl, 5 mM $MgCl_2$, and 0.25 mM ATP).

For investigating the role of FH1 domain on profilin-actin polymerization, 3 μM actin or profilin-actin (molecular ratio 4:1) was polymerized in the presence of 120 nM AtFH8(FH1FH2) or AtFH8(FH2) by adding 1/10 volume of 10× F-buffer.

For depolymerization assay, F-actin (10 μM) was mixed with or without AtFH8(FH1FH2), incubated at room temperature for 1 h and diluted to 0.1 μM into F-buffer. The polymerization and depolymerization dynamics were measured by 90° light scattering with fluorescence spectrophotometer (Fluoro Max-2, Instruments SA, Edison, NJ) set for excitation and emission wavelengths of 450 nm, as described by Cooper and Pollard (1982).

Determination of Critical Concentration for Actin Polymerization

For Cc determination, various concentrations of G-actin were polymerized in 1× F-buffer in the absence or presence of 80 nM AtFH8(FH1FH2) for 16 h at room temperature. The light scattering values of F-actin at each concentration at the beginning (F0) and after the 16 h polymerization (F16) was measured, respectively. The light scattering value from G-actin at each concentration was made as a control. The net increase in light scattering ([F16 − F0] − [G16 − G0]) was plotted against the actin concentration, and the Cc was obtained by adding a linear trend line to the data points and by determining the intercept on the *x* axis.

Barbed-End Elongation Rate Assay

Preformed actin filaments (10 μM) were mixed with equal volume of 10 μM unlabeled phalloidin and sheared 6 times through number 4 gauge needle to generate actin filaments seeds. Then, 70 μL actin filaments seeds were mixed with 70 μL AtFH8(FH1FH2) in 3 × F-buffer. After incubation for 5 min, 140 μL of 1 μM G-actin or profilin-actin (molecular ratio 4:1) was added to the mixture. After mixing by pipetting, the light scattering was recorded for 3 min and the initial elongation rate was measured as the slope of the increase of the light scattering.

Actin Filament Binding Assays

Different concentrations of actin (final volume of 100 μL) were polymerized for 16 h at 4°C in F-buffer. Then AtFH8(FH1FH2) was added to each sample to a final concentration of 0.2 μM followed by gentle flicking. After

incubation for 30 min on ice, all samples were centrifuged at 200,000*g* for 45 min at 4°C in a TLA-110 rotor (Beckman, Fullerton, CA). A total of 80 μL supernatant was removed and 20 μL 5× SDS-PAGE sample buffer added. After removal of the remaining supernatant, pellets were resuspended in 100 μL 1× SDS-PAGE sample buffer. Supernatants and pellets were analyzed with Coomassie-Blue stained SDS-PAGE.

For determination of apparent *K*d of AtFH8(FH1FH2) with actin filaments, the AtFH8(FH1FH2) bands were quantified by a densitometry using Glyko Bandscan software (Glyko, Novato, CA). The relative OD value of AtFH8(FH1FH2) of the supernatants and the pellets were plotted against actin concentrations using the Graphpad prism v.4.0 (Graphpad Software, San Diego). The intersection of the 2 lines indicates that 50% of AtFH8(FH1FH2) binds to actin filaments.

Profilin-Sepharose Binding Assay

Recombinant human profilin I was overexpressed in *E. coli* (kindly provided by C. Staiger, Purdue University) and purified using Poly-L-Pro affinity chromatography, as described previously (Karakesisoglou et al., 1996). Purified profilin was conjugated to CNBr-activated Sepharose 4B (Amersham Biosciences, Uppsala), according to the methods of Rozycki et al. (1991).

A total of 5 μM AtFH8(FH1FH2) or AtFH8(FH2) was incubated with 300 μL of immobilized profilin after washing 3 times with G-buffer, and the beads were eluted with 7 M urea and spun down at 1,000*g* for 1 min. The saved supernatants were analyzed by SDS-PAGE, in which actin and BSA were included as controls.

Fluorescence Microscopy of Actin Filaments

A total of 2 μM actin or profilin-actin (molecular ratio 4:1) in the presence or absence of AtFH8 truncated proteins was polymerized by the addition of 1/10 volume of 10× F-buffer. At the time point of 5 min, all samples were examined immediately by fluorescence microscopy. Actin filaments were labeled with Alexa-phalloidin by diluting 3 μL of actin filaments with 2 μL 3.3-μM labels. After diluting with additional 45 μL F-buffer, approximately 5 μL was applied to coverslips and observed on a laser scanning confocal microscope (Olympus IX70, Tokyo).

For severing assay of AtFH8(FH1FH2) to actin filaments, actin (3 μM) was polymerized for over 16 h at 4°C in F-buffer. Then AtFH8(FH1FH2) or AtFH8(FH1FH2) dialysis buffer was added to the polymerized actin (30 nM final) and mixed by gentle pipetting, then incubated for 1 h. A 3-μL sample was moved to a new tube, and 2 μL F-buffer containing phalloidin (6.6 μM) was added and incubated for 5 min at 4°C. Then the sample was diluted 20-fold with F-buffer and then observed on fluorescence microscope.

Construction of Overexpression Vector and Arabidopsis Transformation

To investigate the role of AtFH8 in phenotype changes of Arabidopsis and the organization of actin cytoskeleton in vivo, we overexpressed this gene in wild-type plants and GFP-tagged-mTalin transgenic plants that express a green fluorescent talin fusion protein (GFP-mTalin) that binds specifically to filamentous-actin, respectively (McKann and Craig, 1997; Kost et al., 2000), to examine if AtFH8 leads to other phenotype changes or affects the actin filament networks. The coding region of AtFH8 was amplified using pGEM-AtFH8 plasmid as a template. Then the product was cloned into pCAMBIA1300 under the control of the superpromoter. The constructed pCAMBIA1300-AtFH8 was introduced into Arabidopsis via *Agrobacterium tumefaciens*-mediated transformation by the floral dip method. Transformed plants were selected by resistance to hygromycin and the presence of the transgene was confirmed by PCR of genomic DNA using transgene-specific primers.

Then T_1 plants positive for the presence of the transgene were determined to be hemizygous or homozygous by the segregation ratios of hygromycin-resistant T_2 progeny. Four T_1 plants showing uniform hygromycin sensitivity in T_2 progeny were verified for gene overexpression level by RT-PCR, and lines with high transgene expression levels were selected for phenotype analysis.

Root Hair Observation

Seedlings were grown on Murashige and Skoog buffer with 0.7% agar (w/v) plates, which were placed vertically to allow root growing along the agar surface in the cultivating condition described above. On day 5 after germination, the seedlings of wild-type or AtFH8-overexpressing homozygote were placed on slides and viewed under a microscope (Olympus) equipped with a digital camera (SpotII Diagngstic Instruments, Japan). The root hairs in the 1-mm length region at the midpoint of a root were focused and photographed. From this region, 10 fully expanded root hairs (all >40 μm) were randomly selected for their length measurement (Rahman et al., 2002). Meanwhile, the number of root hairs <40 μm was counted from the same zone. The root hair length data were generated from the root hair photographs using software AutoCAD 2005 (Autodesk) and converted to micrometers by comparison with a scaled slide. Values from 8 roots of each type were used to determine the mean for root hair length and <40 μm hair numbers. The abnormal phenotypes of AtFH8-overexpressing root hairs were imaged from the whole hairs rather than special regions.

Observations of F-Actin Structures in Root Hair Cells

AtFH8/GFP-mTalin transgenic Arabidopsis lines have been used to visualize actin filaments in living root hair cells. Seeds of AtFH8/GFP-mTalin homozygote plants and the wild-type/GFP-mTalin plants were sterilized, then vernalized for 3 d and grown on Murashige and Skoog plates. Whole root organ from 8-d-old seedlings was mounted in water, and F-actin organization in root hair cell was observed under a confocal microscope (Olympus IX70). GFP fluorescence was excited with the 488-nm line of the argon laser. Four lines of AtFH8/GFP- mTalin were examined.

ACKNOWLEDGMENTS

We thank Dr. Ming Yuan (China Agricultural University, China) for wild-type/GFP-mTalin transgenic Arabidopsis lines, Dr. Zhizhong Gong (China Agricultural University, China) for pCAMBIA1300 vector, Dr. Christopher, J. Staiger (Purdue University) for profilin expression vector, and Dr. Noni Franklin-Tong for critical reading.

Received October 26, 2004; revised January 5, 2005; accepted January 24, 2005, published May 27, 2005.

LITERATURE CITED

Alberts AS (2001) Identification of a carboxyl-terminal diaphanous-related formin homology protein autoregulatory domain. J Biol Chem **276:** 2824–2830

Ayscough KR (1998) *In vivo* function of actin binding proteins. Curr Opin Cell Biol **10:** 102–111

Baluska F, Sala J, Mathu J, Braun M, Jaspe F, Samaj J, Chua NH, Barlow PW, Volkmann D (2000) Root hair formation: F-actin-dependent tip growth is initiated by local assembly of profilin-supported F-actin meshworks accumulated within expansin-enriched bulges. Dev Biol **227:** 618–632

Banno H, Chua NH (2000) Characterization of the *Arabidopsis* formin-like protein AFH1 and its interacting protein. Plant Cell Physiol **41:** 617–626

Braun M, Baluska F, von Witsch M, Menzel D (1999) Redistribution of actin, profilin and phosphatidylinositol-4,5-bisphosphatein growing and maturing root hairs. Planta **209:** 435–443

Cheung AY, Wu H (2004) Overexpression of an Arabidopsis formin stimulates supernumerary actin cable formation from pollen tube cell membrane. Plant Cell **16:** 257–269

Cooper JA, Buhle EL Jr, Walker SB, Tsong TY, Pollard TD (1983) Kinetic evidence for a monomer activation step in actin polymerization. Biochemistry **22:** 2193–2202

Cooper JA, Pollard TD (1982) Methods to measure actin polymerization. Methods Enzymol **85:** 182–210

Cooper JA, Pollard TD (1985) Effect of capping protein on the kinetics of actin polymerization. Biochemistry **24:** 793–799

Cvrčková F (2000) Are plant formins integral membrane proteins? Genome Biol **1:** 1–7

Cvrčková F, Novotný M, Pícková D, Žárský V (2004) Formin homology 2 domains occur in multiple contexts in angiosperms. BMC Genomics **5:** 44

Deeks MJ, Hussey PJ, Davies B (2002) Formins: intermediates in signal-

transduction cascades that affect cytoskeletal reorganization. Trends Plant Sci **7:** 1360–1385

Dolan L, Duckett CM, Grierson C, Linstead P, Schneider K, Lawson E, Dean C, Poethig S, Roberts K (1994) Clonal relationships and cell patterning in the root epidermis of *Arabidopsis*. Development **120:** 2465–2474

Evangelista M, Blundell K, Longtine MS, Chow CJ, Adames N, Pringle JR, Peter M, Boone C (1997) Bni1p, a yeast forming linking cdc42p and the actin cytoskeleton during polarized morphogenesis. Science **276:** 118–122

Evangelista M, Zigmond S, Boone C (2003) Formins: signaling effectors for assembly and polarization of actin filaments. J Cell Sci **116:** 2603–2611

Favery B, Chelysheva LA, Lebris M, Jammes F, Marmagne A (2004) Arabidopsis formin AtFH6 is a plasma membrane-associated protein upregulated in giant cells induced by parasitic nematodes. Plant Cell **16:** 2529–2540

Fu Y, Wu G, Yang Z (2001) Rop GTPase-dependent dynamics of tip-localized F-actin controls tip growth in pollen tubes. J Cell Biol **152:** 1019–1032

Geitmann A, Emons AM (2000) The cytoskeleton in plant and fungal cell tip growth. J Microsc **198:** 218–245

Harris ES, Li F, Higgs HN (2004) The Mouse formin, FRLα, slows actin filament barbed end elongation, competes with capping protein, accelerates polymerization from monomers, and severs filaments. J Biol Chem **279:** 20076–20087

Hellman U, Wernstedt C, Gonez J, Heldin CH (1995) Improvement of an ''in-gel'' digestion procedure for the micropreparation of internal protein fragments for amino acid sequencing. Anal Biochem **224:** 451–455

Huang S, Blanchoin L, Kovar DR, Staiger CJ (2003) Arabidopsis capping protein (AtCP) is a heterodimer that regulates assembly at the barbed ends of actin filaments. J Biol Chem **278:** 44832–44842

Jones MA, Shen JJ, Fu Y, Li H, Yang Z, Grierson CS (2002) The Arabidopsis Rop2 GTPase is a positive regulator of both root hair initiation and tip growth. Plant Cell **14:** 763–776

Karakesisoglou I, Schleicher M, Gibbon BC, Staiger CJ (1996) Plant profilins rescue the aberrant phenotype of profilin-deficient dictyostelium cells. Cell Motil Cytoskeleton **34:** 36–47

Kost B, Lemichez E, Spielhofer P, Hong Y, Tolias K, Carpenter C, Chua NH (1999) Rac homologues and compartmentalized phosphatidylinositol 4,5-bisphosphate act in a common pathway to regulate polar pollen tube growth. J Cell Biol **145:** 317–330

Kost B, Spielhofer P, Mathur J, Dong CH, Chua NH (2000) Non-invasive F-actin visualization in living plant cells using a GFP-mouse talin fusion protein. *In* CJ Staiger, F Baluska, D Volkmann, PW Barlow, eds, Actin: A Dynamic Framework for Multiple Plant Cell Functions. Kluwer Academic, Dordrecht, The Netherlands, pp 637–659

Kovar DR, Kuhn JR, Tichy AL, Pollard TD (2003) The fission yeast cytokinesis formin Cdc12p is a barbed end actin filament capping protein gated by profilin. J Cell Biol **161:** 875–887

Li F, Higgs HN (2003) The mouse formin mDia1 is a potent actin nucleation factor regulated by autoinhibition. Curr Biol **13:** 1335–1340

Marchler-Bauer A, Anderson JB, DeWeese-Scott C, Fedorova ND, Geer LY, He S, Hurwitz DI, Jackson JD, Jacobs AR, Lanczycki CJ, et al (2003) CDD: a curated Entrez database of conserved domain alignments. Nucleic Acids Res **31:** 383–387

McKann RO, Craig SW (1997) The I/LWEQ module: A conserved sequence that signifies F-actin binding in functionally diverse proteins from yeast to mammals. Proc Natl Acad Sci USA **94:** 5679–5684

Miller DD, de Ruijter NCA, Bisseling T, Emons AMC (1999) The role of actin in root hair morphogenesis: studies with lipochito-oligosaccharide as a growth stimulator and cytochalasin as an actin perturbing drug. Plant J **17:** 141–154

Molendijk AJ, Bischoff F, Rajendrakumar CSV, Frim J, Braun M, Gilroy S, Palme K (2001) *Arabidopsis thaliana* Rop GTPases are localized to tips of root hairs and control polar growth. EMBO J **20:** 2779–2788

Ozaki-Kuroda K, Yamamoto Y, Nohara H, Kinoshita M, Fujiwara T, Irie K, Takai Y (2001) Dynamic localization and function of Bni1p at the sites of directed growth in Saccharomyces cerevisiae. Mol Cell Biol **21:** 827–839

Palazzo AF, Cook TA, Alberts AS, Gundersen GG (2001) mDia mediates Rho-regulated formation and orientation of stable microtubules. Nat Cell Biol **3:** 723–729

Pardee JD, Spudich JA (1982) Purification of muscle actin. Methods Cell Biol **24:** 271–289

Pollard TD (1986) Rate constants for the reactions of ATP and ADP-actin with the ends of actin filaments. J Cell Biol **103:** 2747–2754

Pollard TD, Beltzner CC (2002) Structure and function of the Arp2/3 complex. Curr Opin Struct Biol **12:** 768–774

Pring M, Evangelista M, Boone C, Yang C, Zigmond SH (2003) Mechanism of formin-induced nucleation of actin filaments. Biochemistry **42:** 486–496

Pruyne D, Evangelista M, Yang C, Bi E, Zigmond S, Bretscher A, Boone C (2002) Role of formins in actin assembly: nucleation and barbed-end association. Science **297:** 612–615

Rahman A, Hosokawa S, Oono Y, Amakawa T, Goto N, Tsurumi S (2002) Auxin and ethylene response interactions during Arabidopsis root hair development dissected by auxin influx modulators. Plant Physiol **130:** 1908–1917

Ren H, Gibbon BC, Ashworth SL, Sherman DM, Yuan M, Staiger CJ (1997) Actin purified from maize pollen functions in living plant cells. Plant Cell **9:** 1445–1457

Ringli C, Baumberger N, Diet A, Frey B, Keller B (2002) Actin is essential for bulge site selection and tip growth during root hair development of Arabidopsis. Plant Physiol **129:** 1464–1472

Rozycki M, Schutt CE, Lindberg U (1991) Affinity chromatography-based purification of profi1in:actin. Methods Enzymol **196:** 100–118

Sagot I, Klee SK, Pellman D (2002) Yeast formins regulate cell polarity by controlling the assembly of actin cables. Nat Cell Biol **4:** 42–50

Sawin KE (2002) Cell polarity: following forming function. Curr Biol **12:** R6–R8

Soo KO, Han KH, Ryu SB, Kang H (2000) Molecular cloning, expression, and functional analysis of a *cis*-Prenyltransferase from *Arabidopsis thaliana*. J Biol Chem **275:** 18482–18488

Staiger CJ (2000) Signalling to the actin cytoskeleton in plants. Annu Rev Plant Physiol Plant Mol Biol **51:** 257–288

Staiger CJ, Baluska F, Volkman D, Barlow PW, editors (2000) Actin: A Dynamic Framework for Multiple Plant Cell Function. Kluwer Academic Publishers, Dordrecht, The Netherlands

Staiger CJ, Gibbon BC, Kovar DR, Zonia LE (1997) Profilin and actin depolymerizing factor: modulators of actin organization in plants. Trends Plant Sci **2:** 275–281

Tolliday N, VerPlank L, Li R (2002) Rho1 directs formin-mediated actin ring assembly during budding yeast cytokinesis. Curr Biol **12:** 1864–1870

Valenta R, Duchêne M, Pettenburger K, Sillaber C, Valent P, Bettelheim P, Breitenbach M, Rumpold H, Kraft D, Scheiner O (1991) Identification of profilin as a novel pollen allergen; IgE autoreactivity in sensitized individuals. Science **253:** 557–560

Volkmann D, Baluska F (1999) Actin cytoskeleton in plants: from transport to signalling networks. Microsc Res Tech **47:** 135–154

Wasserman S (1998) FH proteins as cytoskeletal organizers. Trends Cell Biol **8:** 111–115

Winter D, Podtelejnilov AV, Mann M, Li R (1997) The complex containing actin-related proteins Arp2 and Arp3 is required for the motility and integrity of the yeast actin patches. Curr Biol **7:** 519–529

Zigmond SH (2004) Formin-induced nucleating of actin filaments. Curr Opin Cell Biol **16:** 99–105